Controlled formation and topologies of thiophenolate-based macrocycles: rings, cylinders and bowls

Aase Christensen, Christoph Mayer, Frank Jensen, Andrew D. Bond* and Christine J. McKenzie*

Received 24th August 2005, Accepted 14th October 2005
First published as an Advance Article on the web 7th November 2005
DOI: 10.1039/b512068c

The Schiff-base condensations of 1,3-diaminopropane with a protected thiophenol dialdehyde in the presence of Ni^{2+}, Pd^{2+} or Zn^{2+} can be controlled to yield either mononuclear acyclic, or 2 + 2 and 4 + 4 macrocyclic complexes by the choice of both metal cation and counteranion. The Ni^{2+} complex of the 2 + 2 macrocycle contains two square-planar nickel ions and shows an arrangement similar to one observed previously: the μ-S atoms of the thiophenolate groups are pyramidal and lie on the same side of the plane defined by the four N atoms of the macrocycle to give a V-shaped molecule. By contrast, the Zn^{2+} complex of the 2 + 2 macrocycle undergoes oligomerisation to yield a bowl-shaped hexanuclear complex that includes a μ_3-carbonate anion. Essential for this topology is the presence of three μ_3-S-thiophenolato groups that link the three macrocyclic units to form a Zn_3S_3 ring that seals the bottom part of the bowl. In this arrangement, one of the pyramidal μ_3-S atoms in each dinuclear Zn^{2+} complex is inverted relative to the arrangement observed for the dinickel complexes. Molecular modelling suggests that inversion about the μ-S atoms of the 2 + 2 macrocyclic complexes is readily accessible at room temperature and that the contrasting arrangements observed for the Ni^{2+} and Zn^{2+} complexes are those energetically most favourable for the respective metal ions. Rare 4 + 4 macrocyclic complexes are isolated as neutral dinuclear complexes for Ni^{2+} and Pd^{2+} and as a tetranuclear complex cation for Zn^{2+}. The topologies of these systems contrast significantly: those with two square-planar Ni^{2+} or Pd^{2+} ions form extended rings, while that with Zn^{2+} forms a sulfur-lined cylinder which hosts acetonitrile molecules in the crystalline state. Reaction conditions can also be optimised to produce 2 + 1 acyclic ligands as their mononuclear Ni^{2+} and Pd^{2+} complexes, providing potentially useful building blocks for production of more complicated macrocyclic and supramolecular systems.

Introduction

Multi-metallic macrocyclic complexes and metallomacrocycles are of importance in diverse fields such as bioinorganic chemistry and supramolecular chemistry. They find numerous applications, for example in molecular magnetic materials and in metal-ion recognition/binding for environmental purposes. In the last 40 years, considerable work has been undertaken with Schiff-base macrocycles that contain phenolate bridging groups between metal ions.[1] By comparison, the chemistry of the related thiophenolate macrocyclic systems has been less well explored. One expectation is that these macrocycles will show a higher affinity for "soft" transition-metal ions. Mononuclear transition-metal complexes of soft metal ions (*e.g.* Wilkinson's catalyst) are of tremendous importance as stereospecific catalysts in industrial and synthetic organic chemistry. Catalysis by a dipalladium acyclic thiophenolate-based complex with one exchangeable coordination site on each metal ion has been demonstrated.[2] A more recent important result in this area is the report by Heyduk and Nocera[3] who showed that a dinuclear Rh complex catalyses reduction of protons to hydrogen. In general, however, development of effective multinuclear transition-metal complexes as catalysts remains less advanced.

University of Southern Denmark, Department of Chemistry, Campusvej 55, 5230, Odense M, Denmark. E-mail: adb@chem.sdu.dk, chk_chem@chem.sdu.dk; Fax: +45 6615 8780; Tel: +45 6550 2518

The relative paucity to date of thiophenolate macrocyclic systems may be attributed at least in part to synthetic difficulties associated with thiolates, particularly in the presence of redox-active metal ions. Thiolates are generally "non-innocent" ligands with radical states that are readily accessible, especially if they are attached to aromatic systems.[4] In addition, they commonly undergo oxygenation, also while bound to metal ions; such behaviour is observed in the metalloenzyme nitrile hydratase,[5] for example, and also in its model complexes.[6] Sulfur protecting-group chemistry may be used to overcome these synthetic problems to some extent. For example, we,[7] and others,[8,9] have described previously the preparation of dinickel complexes of ditopic macrocycles containing two thiophenolate units (R = CH_3 for the 2 + 2 ligands depicted in Scheme 1). Our study produced the first example of a macrocycle (L_{Me}^{4+4}) containing four thiophenolate units from a 4 + 4 Schiff-base condensation. Further examples of 4 + 4 thiophenolate macrocycles have been reported since by Kersting *et al.*, incorporating amine nitrogen donors rather than imine.[10] These latter compounds were prepared in a stepwise manner, first by linking two thiophenolate dialdehyde moieties *via* an ethylene bridge, then effecting reductive amination between two of these units and four aliphatic diamines, amounting to a 2 + 4 reaction under high-dilution conditions. Metal complexes can be prepared subsequently from the pre-formed macrocycle, and one tetrametallic complex was isolated (Scheme 2). This elegant, but rather more complicated, procedure contrasts to our one-pot 4

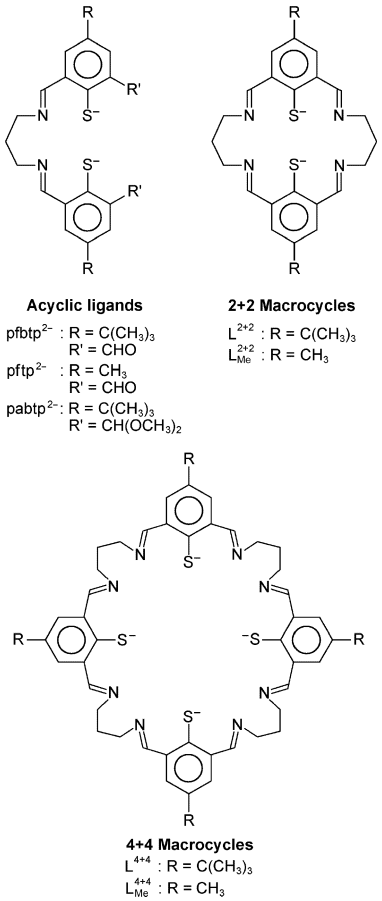

Scheme 1 Ligands produced from metal-ion-templated Schiff-base condensation of 1,3-propanediamine and (*S*)-(2,6-diformyl-4-*tert*-butylphenyl)dimethylthiocarbamate (after removal of the sulfur protecting groups, –CON(CH$_3$)$_2$).

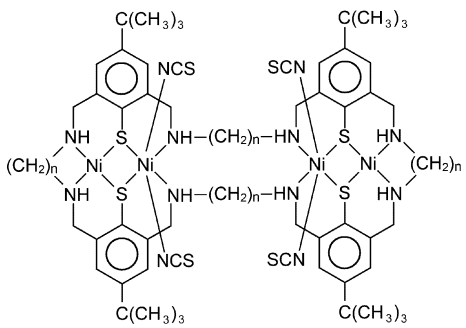

Scheme 2 Tetranickel tetrathiocyanato complex of the tetrathiolate macrocycle prepared by Kersting *et al*. ($n = 2$ or 3).[10]

+ 4 condensation reactions in the presence of metal ions. To our knowledge, the Kersting system and our system are the only known $M_4(SR)_4$ systems in which all the bridging sulfur atoms are part of a single organic ligand. Numerous examples exist in the literature in which thiolate ligands and metal ions form clusters of various nuclearities, with interesting topologies such as cubanes,[11] ladders[12] and cyclized ladders.[13] In general, however, the thiolate donors in these cases originate from separate ligands so that the self-assembly process has many more degrees of freedom compared to the multitopic ligands in which the sulfur atoms are constrained within a single molecule. In this report, we describe further refinements of our one-pot procedure using slightly more soluble homologues of the earlier systems (R = C(CH$_3$)$_3$ for the ligands depicted in Scheme 1). We show that some control can be achieved over the oligomerisation of the thiophenolate building blocks in the presence of transition metal cations, providing multimetallic macrocyclic complexes directly.

Experimental

CAUTION! Although we encountered no problems during preparation of the perchlorate salts, care should be exercised when handling these potentially explosive compounds. Solvents and starting materials were used as supplied from commercial sources and reactions were carried out in air unless otherwise specified.

Syntheses

(*S*)-(2,6-Diformyl-4-*tert*-butylphenyl)dimethylthiocarbamate. 2,6-Diformyl-4-*tert*-butylphenol[14] is reacted with dimethylthiocarbamoyl chloride to give the thiocarbamoyl-protected phenol.[9] This compound undergoes a thermal rearrangement to the desired product by heating 8 g, 0.027 mol at 170 °C under N_2 for 1 h to give a red melt. This is cooled to give a dark solid material, which is dissolved in minimum CH_2Cl_2 (*ca*. 10 mL). EtOH is added until onset of product precipitation and the mixture is left to stand in an open flask. Yield (last step) 61%. Mp 132–133 °C. Anal. Calc. for $C_{15}H_{19}NO_3S$: C, 61.41; H, 6.53; N, 4.77; S, 10.93. Found: C, 61.47; H, 6.58; N, 4.72; S, 11.01%. ^{1}H NMR ($CDCl_3$) δ 1.38 (s, 9H, CH_3), 3.05 (s, 3H, CH_3), 3.25 (s, 3H, CH_3), 8.27 (s, 2H, ArH), 10.57 (s, 2H, CHO). ^{13}C NMR ($CDCl_3$) δ 30.76 ($C(CH_3)_3$), 35.00 ($C(CH_3)_3$), 36.76 (N–CH_3), 36.78 (N–CH_3), 130.75 (ArC), 132.10 (SCN), 138.17 (ArCCHO), 154.37 (ArCC(CH_3)$_3$), 163.91 (ArCS), 190.67 (CHO). FABMS: *m*/*z* 316 ([$C_{15}H_{19}NO_3S$ + Na]$^+$, 12%), 294 ([$C_{15}H_{19}NO_3S$ + H]$^+$, 100%), 221 ([$C_{15}H_{19}NO_3S$ − C_3H_6NO]$^+$, 39%).

[(10,23-Di-*tert*-butyl-13,26-dimercapto-2,6,15,19-tetraaza-1,7,14,20-tetraene[7.7.7.7]metacyclophane)dinickel(II)] diperchlorate, [$Ni_2(L^{2+2})$](ClO_4)$_2$. 1,3-Diaminopropane, (*S*)-(2,6-diformyl-4-*tert*-butylphenyl)dimethylthiocarbamate and Ni(ClO_4)$_2$·6H_2O in (0.4 : 0.2 : 0.2 mmol) dissolved in 3–5 mL of methanol or acetonitrile or MeOH–DMF (1 : 1) mixture was heated to boiling point or *ca*. 100 °C for 15 min. The product crystallized in 30–50% yield as red blocks. Three different crystalline solvates of the same salt were obtained, depending on the solvent system. MALDI MS: *m*/*z* 634 ([$C_{30}H_{38}N_4S_2Ni_2$]$^+$, 100%), 735 ([$C_{30}H_{38}N_4S_2Ni_2(ClO_4)$]$^+$, 25%).

[*N*,*N*′-Propane-1,3-diyl(6-formyl-4-*tert*-butyl-2-methyliminatothiophenolato)]nickel(II), Ni(pfbtp). 1,3-Diaminopropane (0.1315 g, 1.78 mmol) and Ni(ClO_4)$_2$·6H_2O (0.3227 g, 0.88 mmol) were mixed in 5 mL DMF. (*S*)-(2,6-diformyl-4-*tert*-butylphenyl)-dimethylthiocarbamate (0.301 g, 1.03 mmol) in 8 mL DMF was added and the mixture was warmed at *ca* 100 °C for 10 min, during which time the colour changed from olive green to dark brown. The product was deposited as golden brown plates over three days. Yield 203 mg, 43%. Anal. Calc. for Ni(pfbtp), $C_{27}H_{32}N_2O_2S_2Ni$: C, 60.12; H, 5.98; N, 5.19; S, 11.89. Found: C, 60.19; H, 6.03; N, 5.27; S, 11.85%. ^{1}H NMR ($CDCl_3$) δ 1.30 (s,

18H, CH_3), 2.11 (m, 2H, CH_2); 3.99 (t, 4H, CH_2), 7.44 (s, 2H, ArH), 7.89 (s 2H, ArH), 7.91 (s, 2H, imine CH), 10.99 (s, 2H, CHO). ^{13}C NMR ($CDCl_3$) δ 26.57 (2C, $C(CH_3)_4$) 30.87 (6C, CH_3) 34.23 (1C, CH_2) 56.57 (2C, CH_2) 129.70 (2C, Ar) 133.19 (2C, Ar) 135.62 (2C, Ar), 136.03 (2C, Ar), 145.19 (2C, Ar), 146.47 (2C, Ar), 165.20 (2C, imine C), 192.25 (2C, CHO). FABMS: *m/z* 539.0 ([$C_{27}H_{32}N_2O_2S_2Ni$ + Na^+, 100%).

[*N*,*N*-Propane-1,3-diyl(6-formyl-4-*tert*-butyl-2-methyliminato-thiophenolato)]palladium(II), Pd(pfbtp). $PdCl_2$ (34 mg, 0.2 mmol) and 1,3-diaminopropane (45 mg, 0.6 mmol) were mixed in 10 mL DMF and (*S*)-(2,6-diformyl-4-*tert*-butylphenyl)dimethylthiocarbamate (116 mg, 0.4 mmol) in 2 mL DMF was added. The mixture was heated at *ca*. 100 °C for 15 min to give a dark orange solution from which orange crystals of the product were deposited. Yield 38 mg, 57%. MALDI MS: *m/z* 609.0 ([Pd($C_{27}H_{32}N_2O_2S_2$) + Na^+, 100%), 587.0 ([Pd($C_{27}H_{32}N_2O_2S_2$)$^+$, 30%), 627.0 ([Pd($C_{27}H_{32}N_2O_2S_2$) + K^+, 5%).

(10,23,36,49-Tetra-*tert*-butyl-13,26,39,52-tetramercapto-2,6,15,19,28,32,41,45-octaaza-1,7,14,20,27,33,40,46-octaene[7.7.7.7]-metacyclophane)dinickel(II), $Ni_2(L^{4+4})$. A mixture of 1,3-diaminopropane (118 mg, 1.6 mmol) and ammonium chloride (9.7 mg, 0.18 mol) in methanol (10 L) was added to a solution of Ni(pfbtp) (48.1 mg, 0.089 mol) dissolved in 7 mL warm DMF. The mixture was heated under reflux for 15 min and filtered. On standing, the product deposited as a dark brown solid. Yield 30 mg, 58%. Anal. Calc. for $C_{60}H_{76}N_8S_4Ni_2$: C, 62.40; H, 6.63; N, 9.70. Found: C, 61.91; H, 6.78; N, 9.90%. FABMS: *m/z* 1155 ([$C_{60}H_{76}N_8S_4Ni_2$ + H]$^+$, 100%), 1121 ([$C_{60}H_{76}N_8S_4Ni$ + Na + 2H]$^+$, 22%), 528.0 ([$C_{30}H_{38}N_4S_2Ni$ + 2H]$^+$, 30%).

(10,23,36,49-Tetra-*tert*-butyl-13,26,39,52-tetramercapto-2,6,15,19,28,32,41,45-octaaza-1,7,14,20,27,33,40,46-octaene[7.7.7.7]-metacyclophane)dipalladium(II), $Pd_2(L^{4+4})$. (*S*)-(2,6-Diformyl-4-*tert*-butylphenyl)dimethylthiocarbamate (35 mg, 0.12 mmol) in 6 mL DMF was added to a mixture of 1,3-diaminopropane (178 mg, 2.4 mmol) and $PdCl_2$ (21 mg, 0.119 mmol) in 5 mL DMF. The reaction mixture was heated at *ca*. 150 °C for 15 min, during which time the mixture clarified to a dark orange/red. The solution was filtered and allowed to stand, depositing orange crystals over several days. Yield 26 mg, 35%. Anal. Calc. for $C_{60}H_{76}N_8S_4Pd_2{\cdot}3$DMF: C, 56.37; H, 6.66; N, 10.49; S, 8.73. Found: C, 56.32; H, 6.59; N, 10.50, S, 8.69%. FABMS: *m/z* 1250.5 ([$C_{60}H_{76}N_8S_4Pd_2$ + H]$^+$, 47%), 625.0 ([$C_{30}H_{38}N_4S_2Pd$ + H]$^+$, 100%).

(10,23,36,49-Tetra-*tert*-butyl-13,26,39,52-tetramercapto-2,6,15,19,28,32,41,45-octaaza-1,7,14,20,27,33,40,46-octaene[7.7.7.7]-metacyclophane)tetrazinc(II) tetranitrate, $Zn_4(L^{4+4})(NO_3)_4$. A mixture of (*S*)-(2,6-diformyl-4-*tert*-butylphenyl)dimethylthiocarbamate (58 mg, 0.2 mmol) and 1,3-diaminopropane (14.8 mg, 0.2 mmol) in 2 mL methanol was heated at reflux for 15 min during which time the solution changed from orange to red. $Zn(NO_3)_2{\cdot}6H_2O$ (56 mg, 0.2 mmol) in 1 mL methanol was added and the colour changed to an intense yellow. After further heating for 15 min, a solid began to precipitate. All solvent was removed and the residue was dissolved in 5 mL acetonitrile. On standing, crystals of $Zn_4(L^{4+4})(NO_3)_4{\cdot}5CH_3CN$ were deposited. Yield 20 mg, 76%. Anal. Calc. for $C_{60}H_{76}N_{12}S_4O_{12}Zn_4{\cdot}5CH_3CN$: C, 47.98; H, 5.23; N, 13.59. Found: C, 47.45; H, 5.00; N, 11.90%.

Tris[(10,23-di-*tert*-butyl-13,26-dimercapto-2,6,15,19-tetraaza-1,7,14,20-tetraene[7.7.7.7]metacyclophane)dizinc]carbonato tetraperchlorate, $[Zn_6(L^{2+2})_3(CO_3)](ClO_4)_4$. A mixture of (*S*)-(2,6-diformyl-4-*tert*-butylphenyl)dimethylthiocarbamate (47 mg, 0.2 mmol) and 1,3-diaminopropane (14.8 mg, 0.2 mmol) in 3 mL methanol was heated at reflux for 15 min during which time the solution changed from orange to red. $Zn(ClO_4)_2{\cdot}6H_2O$ (74 mg, 0.2 mmol) in 1 mL methanol was added and the colour changed to an intense yellow. The mixture was heated under reflux for 30 min, and yellow crystals of the product were deposited on standing in an open vessel. Yield 29 mg, 45%. ESIMS: *m/z* 324.7 ([$Zn_2(L^{2+2})]^{2+}$, 100%), 501.6 ([$Zn_6(L^{2+2})_3(CO_3)]^{4+}$, 90%), 679.4 ([$Zn_4(L^{2+2})_2(CO_3)]^{2+}$, 95%), 749.0 ([($Zn_2(L^{2+2})$)($ClO_4$)]$^+$, 70%), 1103.6 ({[$Zn_6(L^{2+2})_3(CO_3)$]($ClO_4$)$_2$}$^{2+}$, 8%), 1457.3 ({[$Zn_4(L^{2+2})_2(CO_3)$]($ClO_4$)}$^+$, 6%).

Physical measurements

^{1}H and ^{13}C NMR spectra were recorded on 300 MHz Varian Gemini 2000 instrument, using TMS as an internal reference. IR spectra were measured as KBr discs using a Hitachi 270–30 IR spectrometer. UV-visible absorption spectra were recorded on a Shimadzu UV-3100 spectrophotometer. FAB Mass spectra were recorded on a Kratos MS-50 instrument. MALDI mass spectra were obtained using a 4.7-T Ultima instrument (Ionspec, Irvine, CA), using dihydroxybenzoic acid as matrix. ESI mass spectra were recorded on a Finnigan TSQ 700 MAT triple quadrupole instrument equipped with a nanoelectrospray source. Spectra were obtained by spraying an acetonitrile solution from a coated needle held at 0.8 kV, introduced to the mass spectrometer through a capillary tube heated to 150 °C. Sample concentrations were typically 0.3 mM. Although it may not be explicitly stated, the isotope patterns of all *m/z* assignments have been checked by comparison to the calculated theoretical patterns. Elemental analyses were performed at the Chemistry Department II, Copenhagen University, Denmark and Atlantic Microlab, Inc., Norcross, Georgia, USA.

Single-crystal X-ray diffraction

X-Ray diffraction data for $Pd_2(L^{4+4}){\cdot}3$DMF were collected at 120(2) K using a Siemens SMART CCD diffractometer (Technical University of Denmark). All other diffraction data were collected using a Bruker-Nonius X8APEX-II diffractometer, in most instances at 180(2) K. In the case of $Zn_4(L^{4+4})(NO_3)_4{\cdot}5CH_3CN$, the crystal was cooled further in an effort to enhance the intensity of the diffraction data, but cooling below *ca*. 150 K led to crystal degradation; the reported data collection represents a viable compromise. In all instances, graphite-monochromated Mo-Kα radiation (λ = 0.7107 Å) was used. The structures were solved by direct methods and refined against F^2 using SHELXTL.[15] H atoms bound to C and N atoms were placed geometrically and refined using a riding model. Selected crystallographic data are summarized in Table 1.

The analysis and structure refinement of each nickel complex was straightforward. In the refinement of $[Ni_2(L^{2+2})](ClO_4)_2{\cdot}\frac{1}{2}DMF\cdot\frac{1}{2}CH_3OH$, both solvent molecules were included with 50% site occupancy to provide satisfactory displacement parameters. Partial site occupancy is not a physical requirement—there are no

Table 1 Crystallographic data and details of structure refinements

	$[Ni_2(L^{2+2})](ClO_4)_2{\cdot}2CH_3CN$	$[Ni_2(L^{2+2})](ClO_4){\cdot}\frac{2}{3}CH_3OH$	$[Ni_2(L^{2+2})](ClO_4)_2{\cdot}\frac{1}{2}DMF{\cdot}\frac{1}{2}CH_3OH$	Pd(pfbtp)	$Pd_2(L^{4+4}){\cdot}3DMF$	$Zn_4(L^{4+4})(NO_3)_4{\cdot}5CH_3CN$	$[Zn_6(L^{2+2})_3(CO_3)](ClO_4)_4{\cdot}4H_2O$
Empirical formula	$C_{34}H_{44}Cl_2N_6Ni_2O_8S_2$	$C_{30.67}H_{40.67}Cl_2N_4Ni_2O_{8.67}S_2$	$C_{32}H_{43.5}Cl_2N_{4.5}Ni_2O_9S_2$	$C_{27}H_{32}N_2O_2PdS_2$	$C_{69}H_{97}N_{11}O_3Pd_2S_4$	$C_{70}H_{91}N_{17}O_{12}S_4Zn_4$	$C_{91}H_{122}Cl_4N_{12}O_{23}S_6Zn_6$
M_r	917.19	856.45	887.65	587.07	1469.62	1752.32	2478.39
Crystal system	Monoclinic	Monoclinic	Triclinic	Monoclinic	Monoclinic	Triclinic	Monoclinic
Space group	$I2/a$	$C2/c$	$P\bar{1}$	$C2/c$	$C2/c$	$P\bar{1}$	$P2_1/n$
T/K	180(2)	180(2)	180(2)	180(2)	120(2)	150(2)	180(2)
a/Å	16.3627(9)	20.071(3)	12.373(2)	36.323(4)	34.286(7)	15.567(2)	16.2540(4)
b/Å	11.4598(6)	13.6690(18)	13.331(2)	8.3434(12)	10.232(2)	22.548(2)	46.4678(12)
c/Å	21.3431(14)	40.076(6)	15.212(3)	8.5289(12)	20.489(4)	26.568(2)	16.5610(3)
α/°	90	90	102.565(4)	90	90	107.850(3)	90
β/°	104.445(2)	103.805(7)	100.972(4)	100.795(3)	94.30(3)	103.482(3)	108.158(1)
γ/°	90	90	117.638(4)	90	90	102.425(3)	90
V/Å^3	3875.6(4)	10677(3)	2042.8(6)	2539.0(6)	7168(2)	8207.7(18)	11885.4(5)
Z	4	12	2	4	4	4	4
D_c/Mg m^{-3}	1.572	1.598	1.443	1.536	1.362	1.418	1.385
μ(Mo-Kα)/mm^{-1}	1.275	1.382	1.208	0.923	0.671	1.323	1.453
Total data	22150	26785	17012	4803	35855	65820	43241
Unique data	4928	9431	7118	2083	6324	16884	20184
R_{int}	0.048	0.093	0.042	0.106	0.211	0.149	0.074
$R1$ [$I > 2\sigma(I)$]	0.038	0.051	0.076	0.072	0.216	0.101	0.112
$wR2$ (all data)	0.096	0.125	0.244	0.201	0.476	0.314	0.389
Goodness of fit, S	1.02	0.88	1.04	1.00	2.52	1.07	1.03
ρ_{min}, ρ_{max}/e Å^{-3}	−0.37, 0.62	−0.55, 0.94	−0.88, 2.10	−0.70, 1.09	−14.04, 10.13	−1.10, 1.49	−1.55, 1.82

unacceptable contacts between the solvent molecules—and most likely reflects some degree of solvent loss from the crystal studied. The analysis of Pd(pfbtp) was performed using a plate-like crystal with a minimum dimension of only *ca*. 0.005 mm. The data were weak with only *ca*. 50% observed at the $I > 2\sigma(I)$ level (R_{int} = 0.106) to 0.85 Å resolution. Anisotropic refinement was possible only for Pd, S and N atoms. For $Pd_2(L^{4+4})$·3DMF, the crystal used for data collection was somewhat larger and less isotropic in shape than might be desirable for a Pd^{2+} complex, and the data suffer from severe effects related to anisotropic absorption. Numerous attempts to prepare new crystals to repeat the analysis were unsuccessful. The resulting refinement for $Pd_2(L^{4+4})$·3DMF is therefore of relatively low quality; the data establish connectivity, but do not permit anisotropic refinement. The large peak and hole in the difference electron density are associated with the Pd atom. Analysis of both zinc complexes presented some challenging aspect, largely related to weak diffraction and modelling of diffuse lattice solvent. For $[Zn_6(L^{2+2})_3(CO_3)](ClO_4)_4{\cdot}4H_2O$, the solvent molecules are poorly modelled, but correction *via* a continuous solvent area model[16] is prevented by relatively large voids in the structures coupled with relatively poor data. The C atom of the central carbonate moiety could be refined only with an isotropic displacement parameter. Assignment of this moiety as CO_3^{2-}, rather than NO_3^- for example, was made on the basis of charge balance within the structure, coupled with observation of ions assignable to carbonate-containing complex cations in the ESI-MS data; the X-ray data themselves do not permit definitive distinction between C and N on the basis of bond lengths or displacement parameters. For $Zn_4(L^{4+4})(NO_3)_4{\cdot}5CH_3CN$, the combination of a relatively small crystal and a large primitive unit cell gave rise to weak diffraction which was truncated to 1 Å resolution, with *ca*. 50% observed at the $I > 2\sigma(I)$ level (R_{int} = 0.149). As a result, the structure is of relatively low precision. The two crystallographically distinct complexes were tightly restrained to have comparable geometries and only Zn, S and O atoms were refined anisotropically. The acetonitrile moieties in the lattice were surprisingly well resolved, although the distinction between the N terminus and the CH_3 terminus of each molecule is not clear; the relative orientations of these molecules (in particular those within the cavities of the macrocycles) should be considered highly uncertain.

CCDC reference numbers 282070–282076.

For crystallographic data in CIF or other electronic format see DOI: 10.1039/b512068c

Results and discussion

The Schiff-base condensation reaction of 1,3-diaminopropane and (*S*)-(2,6-diformyl-4-*tert*-butylphenyl)dimethylthiocarbamate, with metal-promoted concurrent sulfur deprotection, in the presence of Ni^{2+}, Pd^{2+} or Zn^{2+} gives four observed products: 1 + 2 acyclic ligands ($pfbtp^{2-}$, $pabtp^{2-}$), a 2 + 2 macrocycle (L^{2+2}) and a 4 + 4 macrocycle (L^{4+4}) (Scheme 1).† The products were characterized as metal complexes: mononuclear complexes of $pfbtp^{2-}$ were isolated for Ni^{2+} and Pd^{2+}; a mononuclear complex of $pabtp^{2-}$ was

† Notably, the analogous 4 + 4 macrocyclic product has not been observed to date for the corresponding Schiff-base adducts of 1,3-diaminopropane and the phenolate analogue, 2,5-phenoldialdehyde.

isolated for Ni^{2+},[17] dinuclear complexes of L^{2+2} were isolated for Ni^{2+}; dinuclear complexes of L^{4+4} were isolated for Ni^{2+} and Pd^{2+}; tetranuclear complexes of L^{4+4} were isolated for Zn^{2+}. In addition, a hexanuclear complex comprising three L^{2+2} units linked by μ_3-thiolate bridges between three of the six metal ions was isolated for Zn^{2+}. Scheme 3 summarizes the synthetic pathways to the isolated compounds. Distinguishing these visibly similar products (for a given metal ion) was not entirely straightforward, since there are

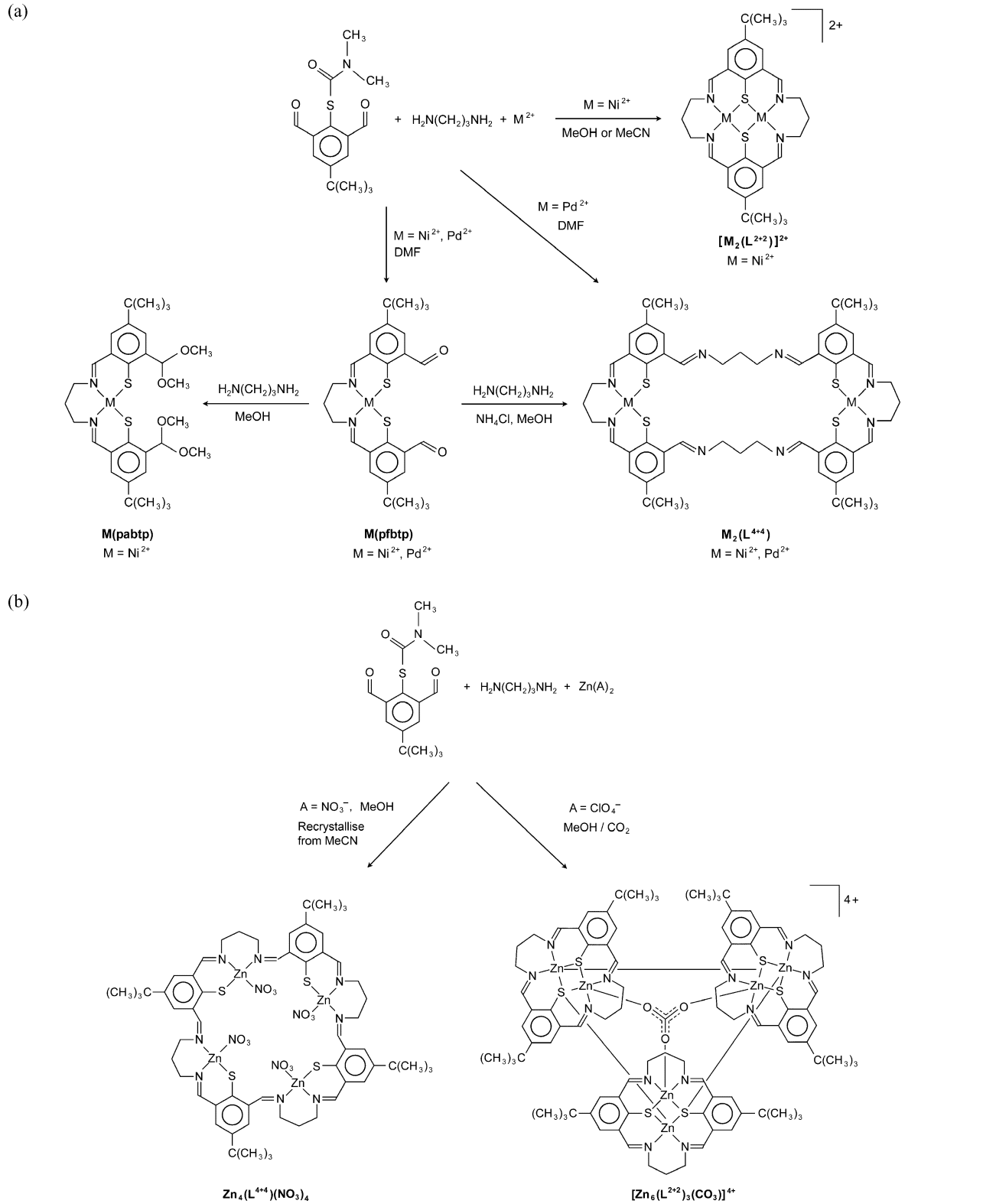

Scheme 3 Summary of the products obtained from Schiff-base condensation of 1,3-diaminopropane with (*S*)-(2,6-diformyl-4-*tert*-butylphenyl)-dimethylthiocarbamate in the presence of divalent ions: (a) reactions with $Ni(ClO_4)_2$ and $PdCl_2$; (b) reactions with $Zn(NO_3)_2$ and $Zn(ClO_4)_2$.

no salient spectroscopic signature differences between L^{2+2}, L^{4+4} and the diacetal 1 + 2 system, pabtp^{2-}. Complexes of the acyclic dialdehyde pfbtp^{2-} are less problematic, being distinguished by a strong band at 1681 cm^{-1} in IR spectra. Mass spectrometry was useful for distinguishing between the mononuclear complexes of pfbtp^{2-} and the dinuclear macrocyclic complexes, but X-ray crystallography was the mainstay for characterization.

Since the original anticipated targets were metal-ion-templated 2 + 2 macrocycles, the three reactants (*S*)-(2,6-diformyl-4-*tert*-butylphenyl)dimethylthiocarbamate, 1,3-diaminopropane and a metal-ion salt were mixed in equimolar proportions in the initial experiments. Only for zinc and nickel were products observed in which the reactants emerge in equimolar proportions.‡ For the reactions incorporating Ni^{2+}, the solvent is an important factor for determining the reaction outcome. In DMF, acyclic Ni(pfbtp) is obtained despite an excess of 1,3-diaminopropane relative to the product. In methanol or acetonitrile, $[Ni_2(L^{2+2})](ClO_4)_2$ is recovered, even in the presence of relatively fewer equivalents of 1,3-diaminopropane. Since imine bond formation is reversible, the principal factor that determines the product may simply be solubility: $[Ni_2(L^{2+2})](ClO_4)_2$ is more soluble than Ni(pfbtp) in DMF, and the reverse is true in methanol and acetonitrile. The dinickel complex of the 4 + 4 macrocycle, $Ni_2(L^{4+4})$, was obtained by reaction of Ni(pfbtp) with 1,3-diaminopropane in methanol, thus amounting to a stepwise synthesis rather than a 4 + 4 ligand assembly. We have no satisfactory explanation for why this reaction occurred most effectively in the presence of ammonium chloride: in the absence of ammonium chloride, the aldehyde groups are converted to methyl acetals and Ni(pabtp) is isolated despite the presence of excess diamine. We note that a related ethyl acetal formation has been observed previously.[18]

The conditions required for isolating Pd(pfbtp) or $Pd_2(L^{4+4})$ differ only marginally in the ratios of the reactants: Pd(pfbtp) is formed by reaction of (*S*)-(2,6-diformyl-4-*tert*-butylphenyl)dimethylthiocarbamate, 1,3-diaminopropane and $PdCl_2$ in 2 : 3 : 1 proportions in DMF (*i.e.* an excess of 1,3-diaminopropane compared to the product stoichiometry), while $Pd_2(L^{4+4})$ is formed from the same reactants in a 1 : 2 : 1 stoichiometry in DMF (*i.e.* an excess of Pd and 1,3-diaminopropane). Both of these compounds are neutral species that can be distinguished by IR spectroscopy and mass spectrometry. The FAB mass spectrum of $Pd_2(L^{4+4})$ shows *m*/*z* 625 ($[(PdC_{30}H_{38}N_4S_2) + H]^+$, 100%) as the major ion, corresponding to half the macrocyclic complex after cleavage of two C–N bonds originating from two different (probably the non-coordinated) 1,3-diaminopropane units. A significant molecular ion is also observed at *m*/*z* 1250.5 ($[(Pd_2C_{60}H_{76}N_8S_4) + H]^+$, 47%). In the spectrum of Pd(pfbtp), the molecular ion is the major peak at *m*/*z* 586, ($[PdC_{27}H_{32}N_2O_2S_2]^+$, 100%).

For the reactions incorporating Zn^{2+}, the outcome is influenced by the identity of the counteranion. This is likely to be attributable to the anion's coordinating ability: nitrate is more strongly coordinating in methanol and acetonitrile than is perchlorate. Thus, if zinc nitrate is used as the starting salt, nitrate remains coordinated to Zn^{2+}, leading to precipitation of a neutral complex $Zn_2(L^{4+4})(NO_3)_4$. In the presence of the less strongly coordinating perchlorate, the 2 + 2 macrocycle is formed, similar to the reactions observed with Ni^{2+} in methanol or acetonitrile. When this reaction mixture is allowed to crystallize slowly under ambient conditions, carbon dioxide is fixed from the atmosphere to form the hexanuclear $[Zn_6(L^{2+2})_3CO_3](ClO_4)_4$. ESI MS (but not MALDI MS) furnishes conditions mild enough to observe the carbonated hexanuclear species (Fig. 1). Monomeric $[Zn_2(L_{Me}{}^{2+2})_2(H_2O)_2]^{2+}$,[19] and dimeric $[Zn_4(L_{Me}{}^{2+2})_2(OH)_2]^{2+}$,[20] have been reported previously, where ($L_{Me}{}^{2+2}$) is the homologous ditopic ligand with R = CH_3 (Scheme 1). The observation here of $[Zn_6(L^{2+2})_3CO_3](ClO_4)_4$ may be considered to extend this series. The pseudo-pH of the reaction will clearly influence the outcome with respect to whether a fifth ligand might be water or hydroxide or consequent carbonate after CO_2 fixation. The fact that the μ_3-carbonato system crystallizes in our case rather than a di-μ-hydroxo system homologous to $[Zn_4(L_{Me}{}^{2+2})_2(OH)_2]^{2+}$, presumably is due to some factor such as concentration of adventitious CO_2.§ It is possible that the presence of *tert*-butyl substituents rather than methyl groups may influence the reaction outcome, although there are no obvious steric constraints in the structure of $[Zn_4(L_{Me}{}^{2+2})(OH)_2]^{2+}$ (*e.g.* between methyl groups) that might prevent formation of the analogous complex with *tert*-butyl groups.

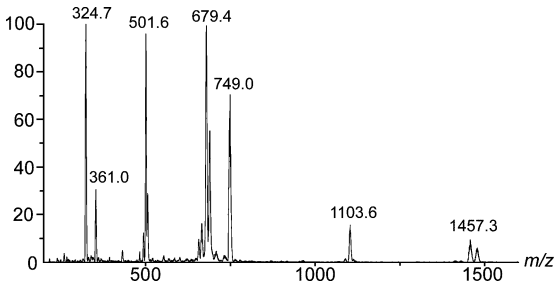

Fig. 1 ESI mass spectrum of $[Zn_6(L^{2+2})_3CO_3](ClO_4)_4$. Assignments: 324.7, $[Zn_2(L^{2+2})(CH_3CN)(H_2O)]^{2+}$; 361.0, $[Zn_2(L^{2+2})]^{2+}$; 501.6, $[Zn_6(L^{2+2})_3(CO_3)]^{4+}$; 679.4, $[Zn_4(L^{2+2})_2(CO_3)]^{2+}$; 749.0, $\{[Zn_2(L^{2+2})](ClO_4)\}^+$; 1103.6, $\{[Zn_6(L^{2+2})_3(CO_3)](ClO_4)_2\}^{2+}$; 1457.3, $\{[Zn_4(L^{2+2})_2(CO_3)](ClO_4)\}^+$.

Crystal structures

$[Ni_2(L^{2+2})](ClO_4)_2\cdot 2CH_3CN$, $[Ni_2(L^{2+2})](ClO_4)_2\cdot\frac{2}{3}CH_3OH$ and $[Ni_2(L^{2+2})](ClO_4)_2\cdot\frac{1}{2}DMF\cdot\frac{1}{2}CH_3OH$. The dinickel(II) complex of the 2 + 2 macrocycle has been characterized as three different crystalline solvates. In addition, a diethyl ether/water solvate has been described previously.[9] In each case, the $[Ni_2(L^{2+2})]^{2+}$ complex displays a "V-shaped" (*syn*) conformation, in which the S atoms of the thiophenolate groups lie to the same side of the plane defined by the four N atoms of the macrocycle (Fig. 2). The dihedral angles between the least-squares planes of the phenyl rings of the thiophenolate units are 83.9(1), 83.4(2)/86.4(1) and 89.2(2)° in the three structures respectively. The conformation of the complex is closely comparable in all three solvated forms: the 28 non-H atoms of the complexes (excluding the C atoms of the CH_3 groups in *tert*-butyl substituents, which are prone to rotational variation) may be overlaid with a maximum rms deviation of only

‡ Where the stoichiometry of the reactions in the Experimental section differ from equimolar, it is because yields were improved using the reported ratios.

§ It is not explicitly stated in ref. 20 whether an inert atmosphere was used in the preparation of $[Zn_4(L_{Me}{}^{2+2})_2(OH)_2]^{2+}$. The presence of CO_2 might be the key difference that leads to production of $[Zn_6(L^{2+2})_3CO_3]^{4+}$ rather than $[Zn_4(L_{Me}{}^{2+2})_2(OH)_2]^{2+}$ in these otherwise similar preparations.

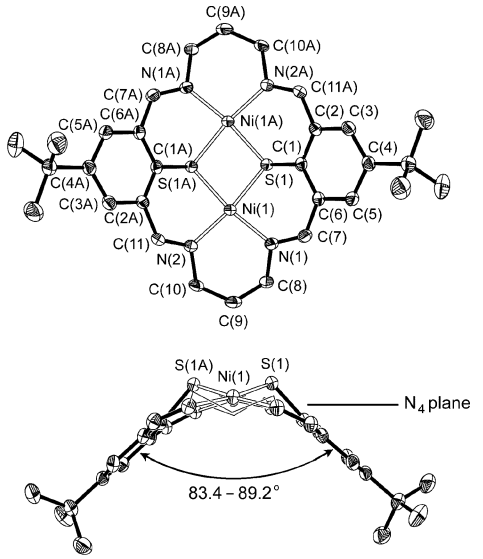

Fig. 2 $Ni_2(L^{2+2})$ complex in $[Ni_2(L^{2+2})](ClO_4)_2{\cdot}2CH_3CN$ showing the *syn* conformation in which the S atoms of the thiophenolate groups lie to the same side of the plane defined by the four N atoms of the macrocycle. Displacement ellipsoids are shown at 50% probability and H atoms are omitted. The $Ni_2(L^{2+2})$ complexes in the other two solvated forms are comparable.

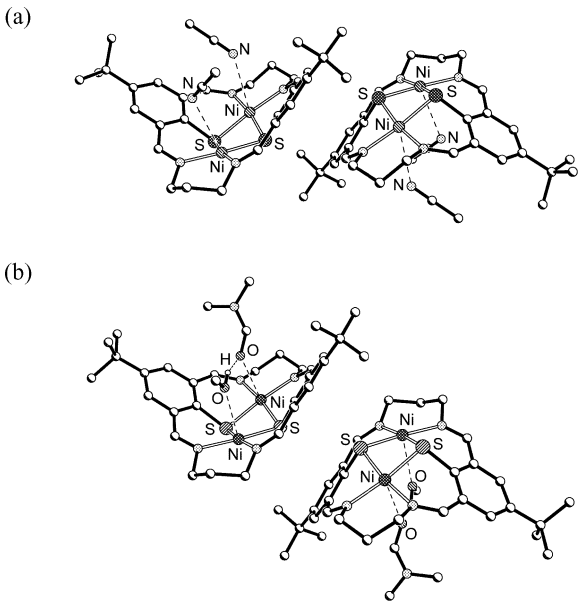

Fig. 3 Back-to-back arrangements of $[Ni_2(L^{2+2})]^{2+}$ in (a) $[Ni_2(L^{2+2})](ClO_4)_2{\cdot}2CH_3CN$ and (b) $[Ni_2(L^{2+2})](ClO_4)_2{\cdot}\frac{1}{2}DMF{\cdot}\frac{1}{2}CH_3OH$. In both cases, the solvent molecules occupy comparable positions on the concave side of the V-shaped $[Ni_2(L^{2+2})]^{2+}$ complexes. H atoms (except in the methanol moiety) and perchlorate anions are omitted.

0.25 Å. In each case, the complexes display approximate C_{2v} point symmetry, with the two-fold axis lying perpendicular to the N_4 plane and passing through the centroid of the complex, and two perpendicular mirror planes passing through the two S atoms and the two Ni atoms, respectively. In the monoclinic structure of $[Ni_2(L^{2+2})](ClO_4)_2{\cdot}2CH_3CN$, the two-fold axis is crystallographic. In $[Ni_2(L^{2+2})](ClO_4)_2{\cdot}\frac{2}{3}CH_3OH$, two independent complexes exist, one lying on the crystallographic two-fold axis and one lying on a general position. In $[Ni_2(L^{2+2})](ClO_4)_2{\cdot}\frac{1}{2}DMF{\cdot}\frac{1}{2}CH_3OH$, the complex lies on a general position.

The crystal structures of $[Ni_2(L^{2+2})](ClO_4)_2{\cdot}2CH_3CN$ and $[Ni_2(L^{2+2})](ClO_4)_2{\cdot}\frac{1}{2}DMF{\cdot}\frac{1}{2}CH_3OH$ show considerable similarity.¶ In each case, adjacent complexes adopt "back-to-back" arrangements in which the phenyl rings of the thiophenolate groups adopt offset face-to-face orientations with interplane separations of *ca* 3.6 Å and their C–S bond vectors lying anti-parallel (Fig. 3). Similar arrangements are observed for the related systems.[8,9] In this arrangement, the *tert*-butyl groups of the thiophenolate rings lie above the Ni_2S_2 centres, effectively preventing further coordination of the Ni^{2+} cations from the convex side of each complex. In each structure, the solvent molecules lie on the concave side. In $[Ni_2(L^{2+2})](ClO_4)_2{\cdot}2CH_3CN$, each acetonitrile molecule is oriented so that its N atom occupies the axial coordination site of a square pyramid about Ni^{2+}, with an Ni···N distance of 3.155(4) Å (Fig. 3(a)). In $[Ni_2(L^{2+2})](ClO_4)_2{\cdot}\frac{1}{2}DMF{\cdot}\frac{1}{2}CH_3OH$, comparable axial sites are occupied either by DMF or by methanol, both moieties being coordinated *via* their O atoms, with Ni···O distances of 2.840(1) and 2.646(2) Å, respectively (Fig. 3(b)). The H atom of the methanol moiety forms a hydrogen bond to the O atom of DMF, approximately parallel to the Ni···Ni vector of the complex. Similar axial interactions with solvent, in these otherwise square-planar nickel complexes, have been noted previously.[9]

In the third solvate, $[Ni_2(L^{2+2})](ClO_4)_2{\cdot}\frac{2}{3}CH_3OH$, adjacent $Ni_2(L^{2+2})$ complexes again adopt back-to-back arrangements. Two distinct arrangements exist, giving rise to two crystallographically distinct complexes. For the complex sited on a general position in the crystal structure, one end forms an arrangement identical to that described previously, *i.e.* thiophenolate groups adopt an offset face-to-face arrangement with their C–S bond vectors lying anti-parallel (as in Fig. 3). This arrangement blocks approach towards one Ni^{2+} cation from the convex side of the $Ni_2(L^{2+2})$ complex. At the other end of the same complex, the thiophenolate groups again adopt face-to-face arrangements, but in this case with their C–S bond vectors lying approximately perpendicular, *i.e.* adjacent complexes are rotated by *ca*. 90° with respect to each other (Fig. 4(a)). This arrangement leaves the convex side of the $Ni_2(L^{2+2})$ complexes exposed, and the perchlorate anions complete an essentially square-pyramidal coordination geometry of the Ni^{2+} cation with Ni···O separations of 2.819(4) Å. The Ni^{2+} cation that has its convex face blocked by the *tert*-butyl group is coordinated by methanol solvent molecules on the concave side, with a Ni···O separation of 2.777(14) Å. This methanol moiety displays some orientational disorder within the concave cavity. The coordination of two methanol molecules per six Ni^{2+} cations (*i.e.* per three $Ni_2(L^{2+2})$ complexes) gives rise to $\frac{2}{3}CH_3OH$ per $Ni_2(L^{2+2})$ in the empirical formula. For the $Ni_2(L^{2+2})$ complex lying on the crystallographic two-fold axis, both of its ends adopt the perpendicular arrangement and both of its Ni^{2+} cations are

¶ The centered monoclinic lattice of $[Ni_2(L^{2+2})](ClO_4)_2{\cdot}2CH_3CN$ can be described by a primitive unit cell $a = 11.460$, $b = 13.042$, $c = 16.038$ Å, $\alpha = 112.42$, $\beta = 110.93$, $\gamma = 116.06°$. This description (although failing to take proper account of the symmetry in the structure) highlights clearly the similarity to the triclinic lattice of $[Ni_2(L^{2+2})](ClO_4)_2{\cdot}\frac{1}{2}DMF{\cdot}\frac{1}{2}CH_3OH$ (see Table 1).

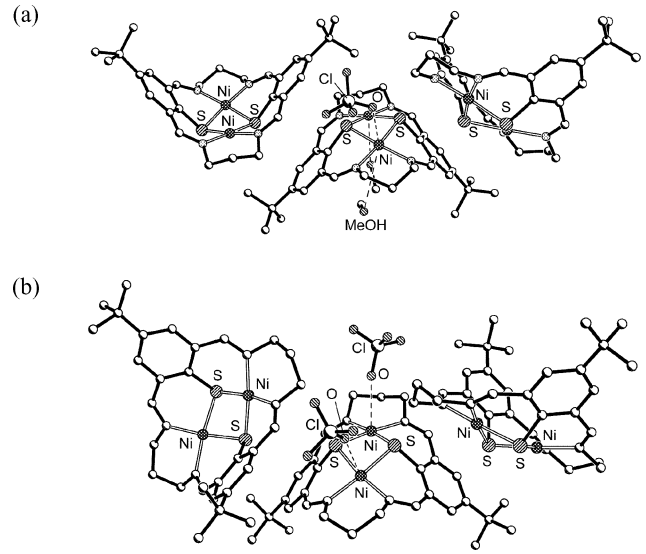

Fig. 4 Environments of the two crystallographically distinct complexes in $[Ni_2(L^{2+2})](ClO_4)_2 \cdot \frac{2}{3}CH_3OH$: (a) at one end of the complex (left), the thiophenolate rings form an offset face-to-face arrangement with the C–S bond vectors lying anti-parallel, while the at the other end (right) the C–S bond vectors lie perpendicular and one Ni atom is further coordinated by a perchlorate moiety; (b) both ends of the complex (related by a crystallographic two-fold rotation axis) adopt the perpendicular arrangement and both Ni atoms are further coordinated by perchlorate moieties. H atoms are omitted.

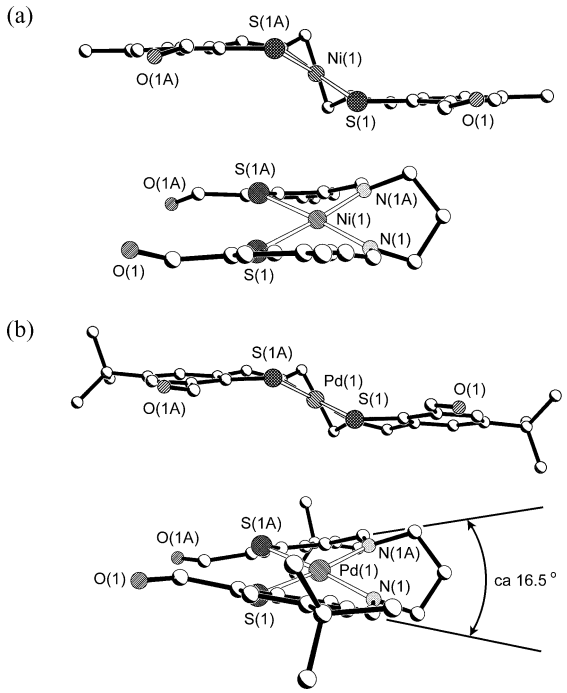

Fig. 5 Metal complexes in (a) Ni(pftp)[7] and (b) Pd(pfbtp) showing projections along the two-fold rotation axis (top) and the direction approximately perpendicular to it, along the long axis of the molecule (bottom). In (a), the planes of the phenyl rings are approximately parallel, while in (b) they form a dihedral angle of 16.5(4)°.

coordinated by perchlorate moieties on the convex side, with equivalent Ni · · · O distances of 2.858(4) Å (Fig. 4(b)).

Pd(pfbtp). The crystal structure of Pd(pfbtp) is closely comparable to that of the Ni^{2+} complex Ni(pftp) ($pftp^{2-}$ = *N*,*N*-propane-1,3-diyl(6-formyl-4-methyl-2-methyliminatothiophenolato, $C_{21}H_{20}N_2O_2S_2$) reported previously.[7] The presence of Pd^{2+} rather than Ni^{2+} in the N_2S_2 coordination site gives rise to subtle changes in the geometry of the complex on account of the differing M–N and M–S bond distances in the two cases. For Ni(pftp), the square-planar geometry of Ni^{2+} coupled with the $(CH_2)_3$ linkage between the two N atoms accommodates an *anti* conformation for the thiophenolate rings (*i.e.* the thiophenolate rings lie on opposite sides of the NiN_2S_2 square plane), with the ring planes approximately parallel (Fig. 5(a)). The complex displays C_2 point symmetry in the solid state, with the two-fold axis passing through Ni and the C atom of the central CH_2 group in the $(CH_2)_3$ linkage. In the Pd^{2+} complex, the relatively longer Pd–N and Pd–S distances impose a slight "twist" on the molecule so that there is a small but discernible distortion of the N_2S_2 unit away from planarity (Fig. 5(b)). The twist is manifested most clearly by the thiophenolate groups, which form a dihedral angle of 16.5(4)° between the least-squares planes of their phenyl rings. The complex retains C_2 point symmetry in the solid state.

In a manner similar to Ni(pftp), the Pd(pfbtp) complexes may be considered to stack along the crystallographic *c* direction. In Ni(pftp), the complexes lie directly one on top of the other (rotated 180° for each adjacent complex), forming Ni · · · Ni separations of 3.96 Å.[7] In Pd(pfbtp), such direct stacking is precluded by the presence of the *tert*-butyl substituents, and adjacent complexes are offset laterally with respect to one another, giving rise to Pd · · · Pd separations of 5.719(2) Å. The offset of adjacent molecules within the stacks is such that the structure in this case might be better described in terms of two-dimensional layers in the *bc* planes, with the long axes of the complexes lying close to perpendicular to the plane of the layers (Fig. 6(a)). The *tert*-butyl groups present an approximately centred rectangular arrangement (defined by the *bc* face of the unit cell) at the surface of each layer (Fig. 6(b)), and adjacent layers stack along the *a* direction so that the *tert*-butyl groups project into the hollows in the surface of the neighbouring layer.

$Pd_2(L^{4+4})\cdot 3DMF$. The crystal structure of $Pd_2(L^{4+4})\cdot 3DMF$ is again closely comparable to the analogous Ni^{2+} complex, $Ni_2(L_{Me}{}^{4+4})\cdot xH_2O$, reported previously.[7] The two Pd^{2+} cations in the complex $Pd_2(L^{4+4})$ occupy opposed coordination sites in the 4 + 4 macrocycle. The complex displays crystallographic C_2 point symmetry with the two-fold axis passing through the centre of the macrocycle, perpendicular to the least-squares plane of the four S atoms (Fig. 7). The two Pd(pfbtp) units within the macrocycle resemble closely those in the crystal structure of Pd(pfbtp) itself: the Pd–S and Pd–N bond distances are comparable, and the phenyl rings of the thiophenolate rings are twisted with respect to each other to form a dihedral angle of 20(1)° between the least-squares planes. The complex as a whole resembles an extended ring, folded *via* the =N–$(CH_2)_3$–N= linkages to form an approximate "V-shaped" conformation. The bending angle of approximately 82° (defined as the dihedral angle between the two PdN_2S_2 square planes) is slightly greater than the 77° angle observed in the comparable Ni^{2+} complex.[7] The non-coordinated =N–$(CH_2)_3$–N= linkages are oriented so that lone pairs associated with N(3)

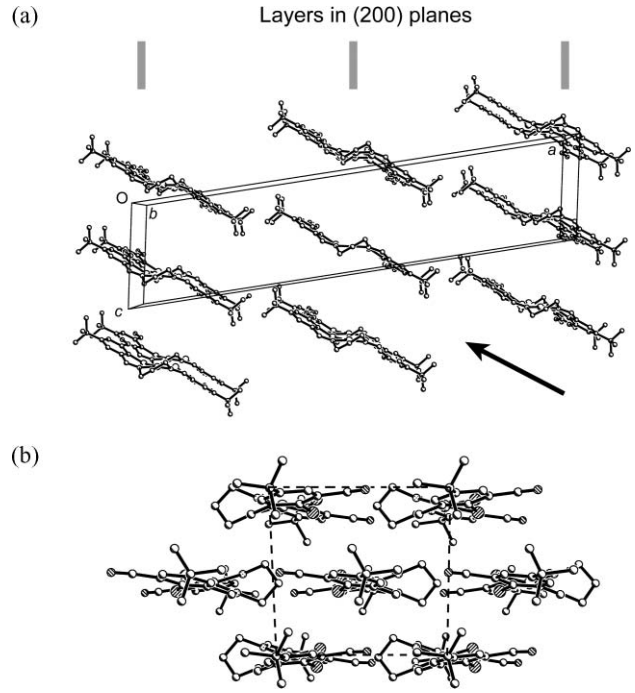

Fig. 6 Packing arrangement in Pd(pfbtp): (a) projection along the *b* direction showing the complexes arranged into layers lying in the (200) planes; (b) projection onto a single layer along the direction indicated by the arrow in (a), showing the offset stacking arrangement of the complexes and the approximate centred rectangular arrangement (defined by the dashed lines) presented by the *tert*-butyl groups on the surface of the layer.

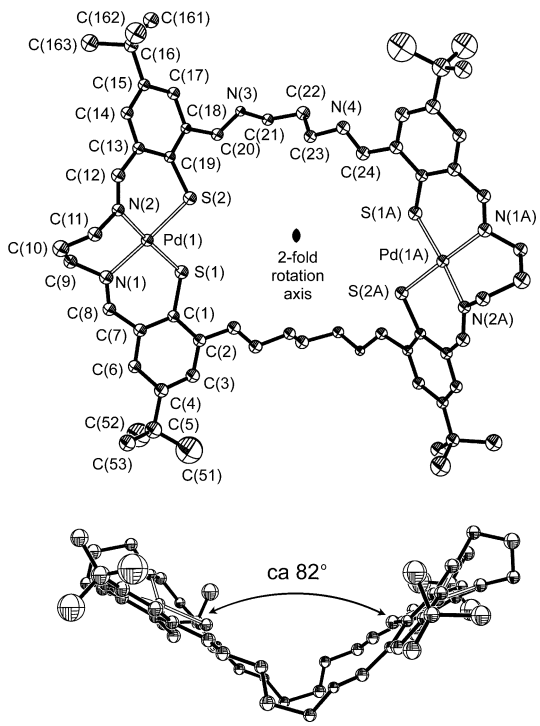

Fig. 7 Perpendicular views of the dinuclear metal complex in $Pd_2(L^{4+4})\cdot 3DMF$, showing the "V-shaped" conformation of the extended ring. H atoms are omitted and only unique C atoms are labelled.

and N(4) may be envisaged to point towards the outside of the macrocycle.

The packing arrangements of $Pd_2(L^{4+4})\cdot 3DMF$ and $Ni_2(L^{4+4})\cdot xH_2O$ are also closely comparable, viewed most clearly in projection along the crystallographic *b* direction, *i.e.* along the two-fold rotation axes of the complexes (Fig. 8). In $Pd_2(L^{4+4})\cdot 3DMF$, adjacent complexes may be considered to be arranged into layers in the (200) planes, with the Pd(pfbtp) portions adopting offset stacked arrangements along *b*. This stacking arrangement is more closely comparable to that observed in Ni(pftp), but with a much larger lateral offset to accommodate the *tert*-butyl substituents, giving rise to Pd···Pd separations of 6.365(3) Å. There is a clear distinction between Pd(pfbtp) portions stacked within layers and the boundary between layers. In $Ni_2(L^{4+4})\cdot xH_2O$, the complexes are translated relative to each other along *a* so that the Ni(pfbtp) portions form more extended two-dimensional arrangements and the distinction between layers is less clear (Fig. 8(b)).[7] This lateral translation gives rise to Ni···Ni separations of 7.53 Å. In $Pd_2(L^{4+4})\cdot 3DMF$, a DMF moiety (displaying some orientational disorder) lies at the centre of each complex, towards the concave side, and further DMF moieties occupy the regions between the layers. The comparable regions are also occupied by solvent molecules

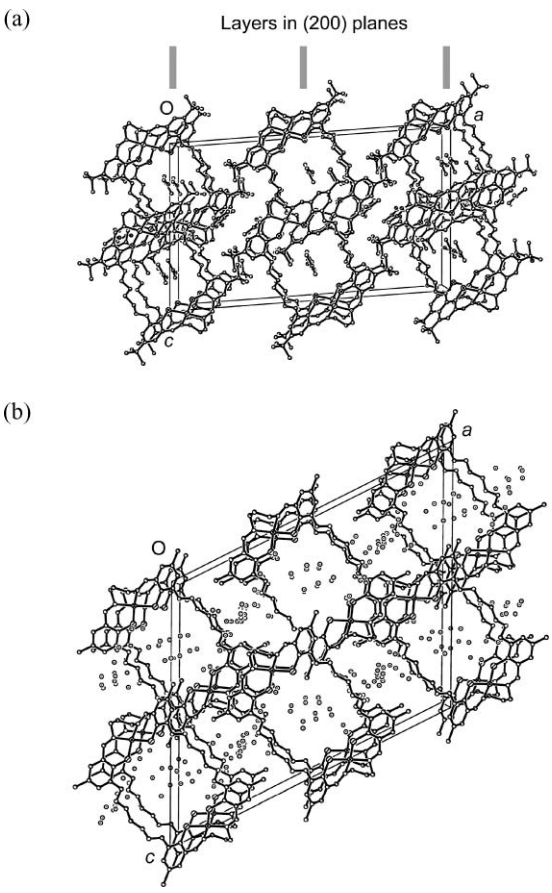

Fig. 8 Packing arrangements in (a) $Pd_2(L^{4+4})\cdot 3DMF$ and (b) $Ni_2(L^{4+4})\cdot xH_2O$. In (a), layers can be clearly distinguished in the (200) planes, while in (b) the complexes are shifted relative to each other along the *a* direction so that the distinction is less clear. The solvent molecules in each case adopt comparable positions.

in $Ni_2(L_{Me}^{4+4})\cdot xH_2O$, although the electron density in that case is diffuse and the identity of the solvent remains somewhat uncertain (modelled as numerous water molecules).[7]

$Zn_4(L^{4+4})(NO_3)_4\cdot 5CH_3CN$. The tetranuclear Zn^{2+} complex of the 4 + 4 macrocycle adopts a conformation dramatically different from those of the dinuclear Ni^{2+} and Pd^{2+} complexes (Fig. 9). The macrocycle is folded to form a cylinder-like arrangement in which the Zn^{2+} cations are coordinated to two N atoms and one S atom, which in this case is not bridging. The cations in each case adopt an essentially tetrahedral coordination geometry, with NO_3^- occupying the fourth coordination site. The nitrate anions form either monodentate or bidentate arrangements. The macrocycle exhibits approximate S_4 point symmetry (although sited on a general position in each crystal structure). The four Zn^{2+} cations lie in a tetrahedral arrangement which is "flattened" along the direction of the approximate S_4 axis. Two crystallographically distinct complexes exist, displaying slightly different conformations. In one complex, two of the Zn^{2+} cations are brought relatively closer together (*ca*. 8.0–8.2 Å) across the macrocycle compared to the other pair (*ca*. 9.2–9.4 Å), so that one end of the cylinder is relatively more open than the other, and the overall arrangement approaches a "bowl". Acetonitrile molecules lie within the "bowl". In the second crystallographically distinct macrocycle, the cross-complex separation between Zn^{2+} cations is comparable (*ca*. 9.1 Å) at both ends, so that the macrocycle resembles more closely a regular cylinder. In this case, two acetonitrile molecules are threaded through the cylinder: thus, the bowl shape can become more cylindrical to accommodate the acetonitrile molecules. Although these CH_3CN molecules are surprisingly well resolved, the X-ray data do not permit definitive distinction between the CH_3 terminus and the N terminus of each molecule, and it is not possible to specify with any confidence the orientations of the CH_3CN molecules within the macrocycle cavity. However, we could speculate that the two N termini are unlikely to be brought into close contact on account of the electrostatic repulsion that would arise between them.

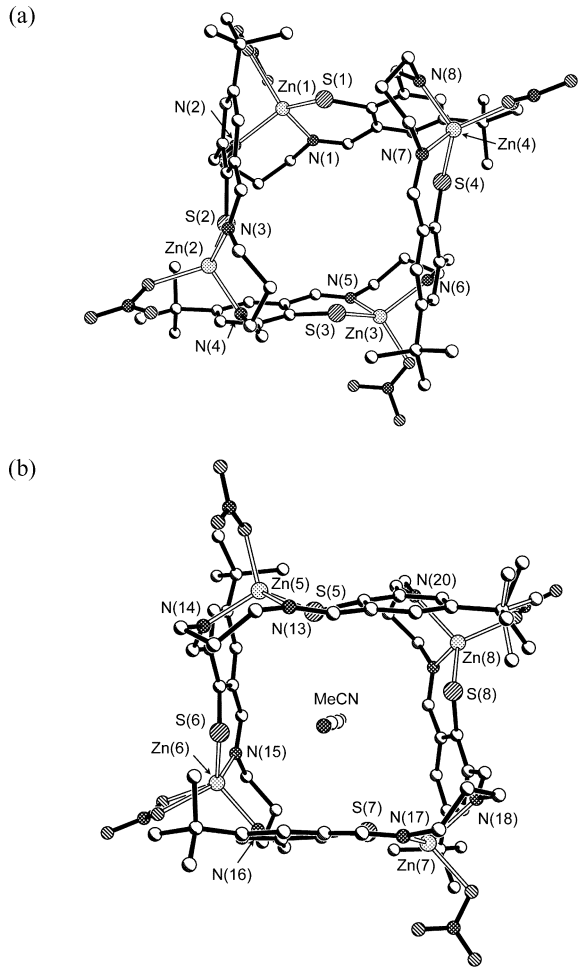

Fig. 9 Two conformations observed for $Zn_4(L^{4+4})(NO_3)_4$: (a) "bowl" shape in which the Zn(1) ··· Zn(3) distance is significantly shorter than the Zn(2) ··· Zn(4) distance. (b) "Cylinder" shape in which the Zn(5) ··· Zn(7) and Zn(6) ··· Zn(8) distances are comparable. The cylinder in (b) is shown with two acetonitrile molecules threaded through it. Acetonitrile molecules also lie within the bowl, but are not shown in (a).

The folding of the macrocycle in $Zn_4(L^{4+4})(NO_3)_4$, compared to the extended ring conformation in the dinuclear Ni^{2+} and Pd^{2+} complexes, can be viewed as a requirement for coordination of the two additional Zn^{2+} cations: a dinuclear complex comparable to that of Ni^{2+} or Pd^{2+} must fold if its previously uncoordinated N atoms are to wrap around the two additional Zn^{2+} cations. It is clear that such an arrangement cannot accommodate a metal cation in a square-planar geometry, which may offer some rationalization for the absence of tetranuclear Ni^{2+} and Pd^{2+} complexes of L^{4+4}. The overall topology of $Zn_4(L^{4+4})(NO_3)_4$, contrasts with that of the only other known tetrametallic complexes of tetrathiophenolate macrocycles, namely the tetranickel system depicted in Scheme 2.[10] This latter system resembles a covalently linked dimer of dinuclear $[Ni_2(L^{2+2})]^{2+}$ moieties, in which the conformation of each dinuclear unit resembles closely that of $[Ni_2(L^{2+2})]^{2+}$ itself.

The packing arrangement of $Zn_4(L^{4+4})(NO_3)_4\cdot 5CH_3CN$ is conveniently considered in terms of 2-D layers parallel to the (001) planes (Fig. 10). Within an individual layer, the macrocycles are arranged so that the cavities through their centres lie either within or perpendicular to the layer plane (Fig. 10(b)). Adjacent macrocycles turned perpendicular to each other interact in a

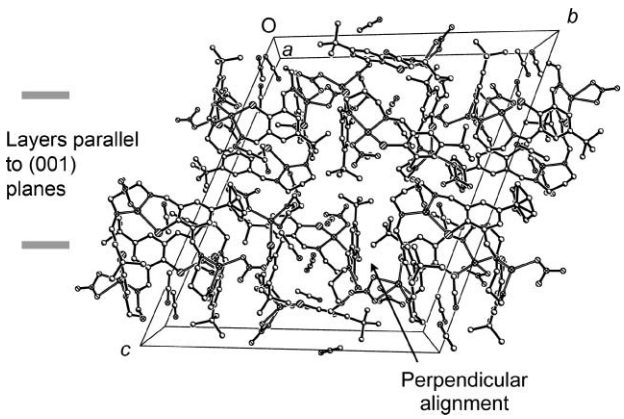

Fig. 10 View along the *a* direction in $Zn_4(L^{4+4})(NO_3)_4\cdot 5CH_3CN$ showing layers parallel to the *ab* face of the unit cell. Macrocycles adopt a perpendicular alignment with their neighbours within layers, and adjacent layers are offset laterally so that there are no channels running through the structure.

manner similar to that seen in the $[Ni_2(L^{2+2})]^{2+}$ complexes: the thiophenolate rings come into face-to-face contact with their C–S vectors approximately perpendicular. The layers are stacked in an *ABAB* manner, offset so that the macrocycles lie perpendicular to their neighbours in adjacent layers. Thus, there are no channels running through the structure and the acetonitrile molecules in the macrocycle cavities are effectively trapped.

$[Zn_6(L^{2+2})_3(CO_3)](ClO_4)_4\cdot 4H_2O$. The hexanuclear complex $[Zn_6(L^{2+2})_3(CO_3)]^{4+}$ consists of three distinct $[Zn_2(L^{2+2})]^{2+}$ units, linked *via* further Zn–S bonds, displaying approximate (non-crystallographic) C_3 point symmetry (Fig. 11). The coordination geometry around three of the six Zn^{2+} cations resembles trigonal bipyramidal, with the two S atoms and two N atoms of a given $[Zn_2(L^{2+2})]^{2+}$ unit occupying two equatorial and two axial positions, and the S atom from an adjacent $[Zn_2(L^{2+2})]^{2+}$ unit occupying one equatorial position. The S atoms of the thiophenolate rings that bridge between these two Zn^{2+} centres adopt μ_3-coordination, in an approximate trigonal-planar arrangement. The three Zn^{2+} cations and three S atoms form a six-membered Zn_3S_3 ring that is approximately planar and very close to three-fold symmetric. The remaining three Zn^{2+} cations lie in second plane, that is close to parallel to the plane of the Zn_3S_3 ring (actual dihedral angle 3.9(1)°), with an approximate perpendicular separation of *ca.* 2.6 Å. The triangular arrangement of these Zn^{2+} cations is distorted, with one Zn ··· Zn distance (4.817(2) Å) significantly longer than the other two (4.450(2) and 4.539(2) Å). The coordination geometry around Zn^{2+} is again approximately trigonal bipyramidal, with the two S atoms and two N atoms of a given $[Zn_2(L^{2+2})]^{2+}$ unit occupying two equatorial and two axial positions. The remaining equatorial coordination site is occupied by O from a μ_3-carbonate anion that lies approximately within the upper Zn_3 plane. The geometry of the three individual $[Zn_2(L^{2+2})]^{2+}$ units in $[Zn_6(L^{2+2})_3(CO_3)]^{4+}$ differs from that observed in the isolated $[Ni_2(L^{2+2})]^{2+}$ units described previously: the S atoms of the thiophenolate groups lie on opposite sides of the plane defined by the four N atoms of the macrocycle, giving rise to an *anti* conformation. The dihedral angles between the least-squares planes of the phenyl rings of the thiophenolate units are 60.1(4), 69.0(4) and 66.4(4)° in the three distinct $[Zn_2(L^{2+2})]^{2+}$ units, respectively. The Zn_3S_3 ring effectively closes one side of the macrocycle, forming the bowl shape within which the carbonate anion lies.

The crystal structure of $[Zn_6(L^{2+2})_3(CO_3)](ClO_4)_4\cdot 4H_2O$ is conveniently described by considering layers in (010) (Fig. 12). Within a given layer, all of the complexes are aligned with their approximate local C_3 axes parallel. In an adjacent layer, related to the primary layer by a centre of inversion, the C_3 axes are also aligned along the same direction, with the bowls adopting a "back-to-back" arrangement. In the adjacent layer on the other side of the primary layer, the bowls are aligned in a side-on manner so that their C_3 axes point in approximately perpendicular directions. The bowls are relatively loosely packed–there are no face-to-face contacts between thiophenolate rings, for example–and the perchlorate anions and water solvent molecules occupy the voids between them.

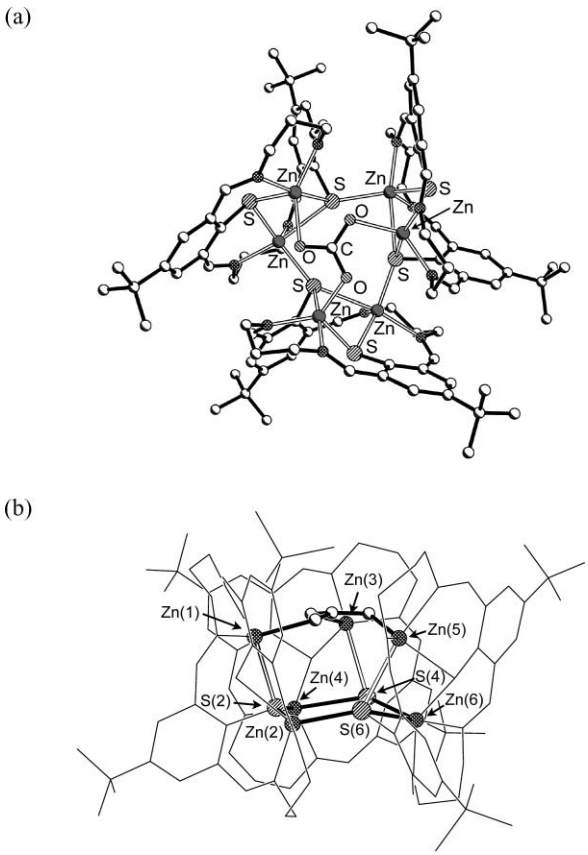

Fig. 11 View of the $[Zn_6(L^{2+2})_3(CO_3)]^{2+}$ complex: (a) along its approximate C_3 rotation axis and (b) perpendicular to it, highlighting the Zn_3S_3 ring in the lower plane and the CO_3^{2-} anion complexed between three Zn^{2+} cations in the upper plane.

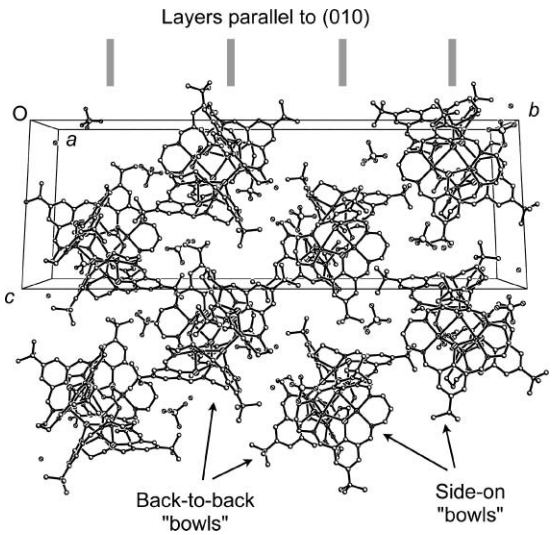

Fig. 12 Perspective view of the crystal structure of $[Zn_6(L^{2+2})_3(CO_3)](ClO_4)_4\cdot 4H_2O$ along the *a* direction showing layers envisaged parallel to the (100) planes. In adjacent layers, the bowl-shaped complexes lie either back-to-back with their neighbour so that their local C_3 axes are parallel, or side-on so that their local C_3 axes are approximately perpendicular.

Modelling studies

In the μ-thiolate bridged systems with L^{2+2}, the two metal ions and the *ipso*-carbon of the phenyl ring are located at three

apices of a tetrahedron around each S atom, with a lone pair of electrons occupying the fourth. Two possibilities exist for the relative orientations of the two tetrahedra in the $[M(L^{2+2})]^{2+}$ macrocyclic complex: a *syn* orientation of the sulfur lone pairs leads to a V-shaped molecule in which both phenyl rings lie on the same side of the N_4 plane of the macrocycle, while an *anti* conformation causes the phenyl rings to lie on opposite sides of the N_4 plane (Scheme 4). Both conformations are observed in the present series. In the discrete dinickel complexes of the 2 + 2 macrocycles[7–9] the *syn* conformation is observed exclusively. In contrast the *anti* orientation is observed in the dinuclear units of $[Zn_6(L^{2+2})_3(CO_3)]^{4+}$ (Fig. 11(a)). Likewise the *anti* conformation was seen in $[Zn_2(L_{Me}{}^{2+2})_2(H_2O)_2]^{2+}$.[19] Both the *syn* and the *anti* conformation are seen in the dimeric $[Zn_4(L_{Me}{}^{2+2})_2(OH)_2]^{2+}$.[20] The question arises as to whether these conformations can interconvert in solution *via* a fluxional sulfur-inversion process. Inversion might occur at one sulfur atom to change the observed conformer, or at both to give an inversion of the entire M_2S_2 core (Scheme 4). These processes could take place by either dissociative or non-dissociative mechanisms. It is well known that thiolate sulfur can invert when attached to a metal centre as a monodentate donor, and when it is part of an organic ring.[21] The possibility of inversion in this system is addressed by considering calculated energies for each of the limiting forms. The coordinates obtained in the structure analysis of $[Ni_2(L^{2+2})]^{2+}$ and a dimeric unit taken from $[Zn_6(L^{2+2})_3(CO_3)]^{4+}$ were used as starting points for the calculations and the structures were fully optimized at the B3LYP level using the 6-31G(d,p) basis set. Both Ni^{2+} and Zn^{2+} were found to favour the geometries observed: for Zn^{2+}, the *syn* conformer is destabilized by approximately 80 kJ mol^{-1} relative to the observed *anti* conformer, while for Ni^{2+}, the *anti* conformer is 50 kJ mol^{-1} less stable than the *syn* conformer. In the non-dissociative transition structures, the inverting sulfur atom lies almost in the plane of the surrounding atoms. The activation energy relative to the most stable conformer is calculated to be 105 kJ mol^{-1} for the Zn^{2+} complex and 90 kJ mol^{-1} for the Ni^{2+} complex, indicating that interconversion should occur readily at room temperature.

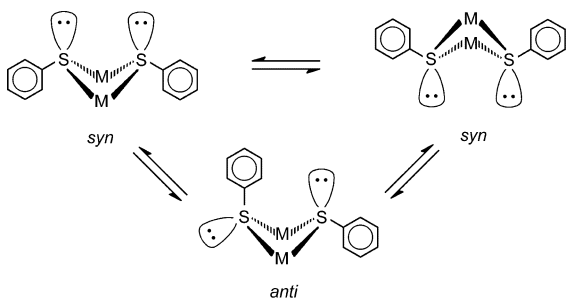

Scheme 4 Conformation arising from a *syn* or *anti* orientation of the S lone pairs in $[M(L^{2+2})]$. For simplicity, only the phenyl rings of the macrocyclic ligand system are drawn.

Conclusions

A series of complexes containing 1,3-diaminopropane, thiophenoldialdehyde and metal-ion building blocks in 1 : 2 : 1, 2 : 2 : 2, 4 : 4 : 2 and 4 : 4 : 4 ratios have been prepared and structurally characterized. The formation of each of these particular entities is influenced by the identity of the metal ion, solvent and counteranions in the synthetic procedure. The rare 4 + 4 thiophenolate macrocycles show dramatically different topologies in their dinuclear and tetranuclear metal complexes. The dinuclear complexes $Ni_2(L^{4+4})$ and $Pd_2(L^{4+4})$ resemble extended rings folded into "V-shaped" conformations, in which the local environment of each square-planar metal ion resembles closely that in the isolated mononuclear complexes, Ni(pftp) and Pd(pfbtp). By contrast, the tetranuclear complex $Zn_4(L^{4+4})(NO_3)_4$, displays a cylindrical conformation that can distort to become more "bowl-like". The cavities within the macrocycle are essentially sulfur-lined rather than metal-lined, presenting the possibility that these systems might be developed as electron-rich hosts for host–guest chemistry. In particular, we intend to investigate the uptake of gases by these materials; we might speculate that the sulfur-lined cavities would show particular affinity for dihydrogen, for example. A hexanuclear complex $[Zn_6(L^{2+2})_3(CO_3)]^{4+}$ is also formed by oligomerisation of three dinuclear 2 + 2 macrocyclic complexes. This complex exhibits a bowl shape, and is occupied by a carbonate anion derived from CO_2 fixation.

Acknowledgements

We are grateful to Dr Inger Søtofte for collecting X-ray diffraction data for $Pd_2(L^{4+4})\cdot 3DMF$ at Technical University of Denmark and to the Danish Natural Science Research Council (SNF) and Carlsbergfondet for provision of the X-ray diffraction equipment. A. D. B. also thanks SNF for funding *via* a Steno stipend. The computational studies were supported by grants from the Danish Center for Scientific Computing to F. J.

References

1 See, for example: B. F. Hoskins, R. Robson and G. A. Williams, *Inorg. Chim. Acta*, 1976, **16**, 121; R. R. Gagne, L. M. Henling and T. J. Kistenmacher, *Inorg. Chem.*, 1980, **19**, 1226; G. A. Williams and R. Robson, *Aust. J. Chem.*, 1981, **34**, 65; H. Diril, H.-R. Chang, Zhang, S. K. Larsen, J. A. Potenza, C. G. Pierpont, H. J. Schugar, S. S. Isied and D. N. Hendrickson, *J. Am. Chem. Soc.*, 1987, **109**, 6207; S. K. Mandal, L. K. Thompson, M. J. Newlands and E. J. Gabe, *Inorg. Chem.*, 1989, **28**, 3707; S. S. Tandon and V. McKee, *J. Chem. Soc., Dalton Trans.*, 1989, 19; S. S. Tandon, L. K. Thompson, J. N. Bridson, V. McKee and A. J. Downard, *Inorg. Chem.*, 1992, **31**, 4635; H. Okawa, J. Nishio, M. Ohba, M. Tadokoro, N. Matsumoto, M. Koikawa, S. Kida and D. E. Fenton, *Inorg. Chem.*, 1993, **32**, 2949.
2 C. J. McKenzie and R. Robson, *J. Chem. Soc., Chem. Commun.*, 1988, 112.
3 A. F. Heyduk and D. G. Nocera, *Science*, 2001, **293**, 1639.
4 D. Herebian, E. Bothe, E. Bill, T. Weyhermuller and K. Wieghardt, *J. Am. Chem. Soc.*, 2001, **123**, 10012; S. Brooker, *Coord. Chem. Rev.*, 2001, **222**, 33; N. D. J. Branscombe, A. J. Atkins, A. Marin-Becerra, E. J. L. MacInnes, F. E. Mabbs, J. McMaster and M. Schroder, *Chem. Commun.*, 2003, 1098.
5 S. Nagashima, M. Nakasako, N. Dohmae, M. Tsujimura, K. Takio, M. Odaka, M. Yohda, N. Kamiya and I. Endo, *Nat. Struct. Biol.*, 1998, **5**, 347.
6 L. Heinrich, Y. Li, J. Vaissermann and J.-C. Chottard, *Eur. J. Inorg. Chem.*, 2001, **40**, 1407; L. A. Tyler, J. C. Noveron, M. M. Olmstead and P. K. Maschrak, *Inorg. Chem.*, 2003, **42**, 5751.
7 A. Christensen, H. S. Jensen, V. McKee, C. J. McKenzie and M. Munch, *Inorg. Chem.*, 1997, **36**, 6080.
8 A. J. Atkins, A. J. Blake and M. Schroder, *J. Chem. Soc., Chem. Commun.*, 1993, 1662; S. Brooker, P. D. Croucher, T. C. Davidson, G. S. Dunbar, C. U. Beck and S. Subramanian, *Eur. J. Inorg. Chem.*, 2000, 169; S. Brooker, P. D. Croucher and F. M. Roxburgh, *J. Chem. Soc., Dalton Trans.*, 1996, 3031.

9 S. Brooker, G. B. Caygill, P. D. Croucher, T. C. Davidson, D. L. J. Clive, S. R. Magnuson, S. P. Cramer and C. Y. Ralston, *J. Chem. Soc., Dalton Trans.*, 2000, 3113.
10 B. Kersting, G. Steinfeld, T. Fritz and J. Hausmann, *Eur. J. Inorg. Chem.*, 1999, 2167; B. Kersting, *Z. Naturforsch., Teil B*, 2000, **55**, 961.
11 A. Xia, M. J. Heeg and C. H. Winter, *J. Organomet. Chem.*, 2003, **37**, 669; D. C. Craig and I. G. Dance,I. G., *Polyhedron*, 1987, **6**, 1157; A.-K. Duhme and H. Strasdeit, *Z. Naturforsch., Teil B*, 1994, **49**, 119.
12 I. G. Dance, M. L. Scudder and L. J. Fitzpatrick, *Inorg. Chem.*, 1985, **24**, 2547; A. J. Banister, W. Clegg and W. R. Gill, *J. Chem. Soc., Chem. Commun.*, 1987, 850; B. Krebs, A. Brommelhaus, B. Kersting and M. Nienhaus, *Eur. J. Solid State Inorg. Chem.*, 1992, **29**, 167; T. C. Deivaraj and J. J. Vittal, *J. Chem. Soc., Dalton Trans.*, 2001, 329.
13 T. Chivers, A. Downard and G. P. A. Yap, *Inorg. Chem.*, 1998, **37**, 5708; T. Kawamoto, N. Ohkashi, I. Nagasawa, H. Kuma and Y. Kushi, *Chem. Lett.*, 1997, 553; D. J. Rose, Y. D. Chang, Q. Chen, P. B. Kettler and J. Zubieta, *Inorg. Chem.*, 1995, **34**, 3973.
14 H. R. Chang, S. K. Larsen, P. D. W. Boyd, C. G. Pierpont and D. N. Hendrickson, *J. Am. Chem. Soc.*, 1988, **110**, 4565–76.
15 G. M. Sheldrick, *SHELXTL v. 6.10*, Bruker AXS, Madison, WI, USA, 2000.
16 P. v. d. Sluis and A. L. Spek, *Acta Crystallogr., Sect. A*, 1990, **46**, 194; implemented as the *SQUEEZE* procedure in A. L. Spek, *PLATON, A Multipurpose Crystallographic Tool*, Utrecht University, Utrecht, The Netherlands, 1998.
17 J. K. Bjernemose, C. J. McKenzie, P. R. Raithby and S. J. Teat, *Acta Crystallogr., Sect. E*, 2004, 1841.
18 S. Brooker and P. D. Croucher, *J. Chem. Soc., Chem. Commun.*, 1995, 1493.
19 S. Brooker, P. D. Croucher and F. M. Roxburgh, *J. Chem. Soc., Dalton Trans.*, 1996, 3031.
20 N. D. J. Branscombe, A. Blake, A. Marin-Becerra, W.-S. Li, S. Parsons, L. Ruiz-Ramirez and M. Schroder, *Chem. Commun.*, 1996, 2573.
21 S. S. Oster and W. D. Jones, *Inorg. Chim. Acta*, 2004, **357**, 1836; P. Haake and P. C. Turley, *J. Am. Chem. Soc.*, 1967, **89**, 4611.

